







Nano-ZnO catalyzed microwave synthesis of novel α -aminophosphonates: anti-diabetic potential via molecular docking, ADMET analysis, and α -amylase and α -glucosidase inhibition studies

A. Hanumantha Rao ^{1,2*}, Ch. Subramanyam ¹, K. Venkata Ramana ³,
C. Gladis Raja Malar ⁴, G.R. Satyanarayana ⁵
and V. Madhava Rao* ¹

¹Department of Chemistry (recognized as research centre by A.N. University), Bapatla Engineering College (Autonomous), Bapatla, Andhra Pradesh, India -522101

²Department of Chemistry, Acharya Nagarjuna University, Guntur, Andhra Pradesh, India -522510

³Department of Humanities & Sciences, KSRM College of Engineering, Kadapa-516005

⁴Department of Chemistry, Vel Tech Multi Tech Dr.Rangarajan Dr.Sakunthala Engineering College, Avadi, Chennai, Tamil Nadu, India-600062

⁵Department of Chemistry, Sir CR Reddy College, Eluru, Andhra Pradesh, India -534007

(Received January 21, 2025; Revised March 31, 2025; Accepted April 07, 2025)

Abstract: A more efficient and environmentally friendly approach has been developed for synthesizing α -aminophosphonates through the Kabachnik-Fields (K-F), catalyzed by nano-ZnO in a solvent-free environment, utilizing microwave irradiation. Before synthesis, each compound underwent *in silico* ADMET analysis and molecular docking to assess drug-like characteristics and their potential to inhibit α -amylase. The structure of the newly synthesized compounds was validated using spectroscopic analysis, and their *in vitro* inhibitory effects on α -amylase and α -glucosidase were assessed. Among the compounds **8g** (IC₅₀, 99.2±0.5 µg/mL), **8i** (IC₅₀, 101.2±0.3 µg/mL), **8e** (IC₅₀, 102.1±0.4 µg/mL) and **8j** (IC₅₀, 103.4±0.4 µg/mL) containing anthracen-9-ylamino, phenanthren-9-ylamino, 2-oxo-2H-chromen-6-yl)amino and 2-benzoylphenyl)amino moieties respectively, exhibited the highest inhibitory activity on α -amylase, superior to the reference compound acarbose (IC₅₀, 104.5±0.1 µg/mL). The remaining compounds demonstrated moderate to good enzyme inhibition. **8c** bearing with 4-fluorophenyl substituent (IC₅₀, 88.4±0.7 µg/mL), **8e** (IC₅₀, 90.0±0.4 µg/mL) bearing with 2-oxo-2H-chromen-6-yl substituent and **8d** (IC₅₀, 91.1±0.9 µg/mL) bearing with 2-methylbenzo[d]oxazol-5-yl moiety have shown the highest inhibitory activity on α -glucosidase than the reference drug, Acarbose ((IC₅₀, 93.1±0.8 µg/mL). The remaining compounds exhibited moderate to good inhibition on the enzyme with IC₅₀ ranging 94.5±0.9 to 141.4±0.7 µg/mL.

Keywords: Kabachnik-Fields (K-F) reaction; nano-ZnO; microwave irradiation; molecular docking; α -amylase; α -glucosidase. © 2025 ACG Publications. All rights reserved.

* Corresponding author: E-mail: vmrgpm@gmail.com

The article was published by ACG Publications

<https://www.acgpubs.org/journal/organic-communications> Month-Month 202x EISSN:1307-6175

DOI: <http://doi.org/10.25135/acg.oc.187.2501.3413>

Available online: April 29, 2025

1. Introduction

Diabetes is a chronic condition that occurs when there is insufficient insulin production by the pancreas or when the body fails to utilize the produced insulin effectively. One approach to managing early-stage diabetes involves reducing postprandial hyperglycemia. The metabolism of carbohydrates depends on the enzymes α -amylase and α -glucosidase. While α -glucosidase transforms these oligosaccharides into absorbable monosaccharides like glucose, α -amylase breaks down starch into smaller oligosaccharides. By slowing down the breakdown of carbohydrates, these enzymes reduce postprandial hyperglycemia by releasing glucose into the bloodstream gradually and under control. This is attained by inhibiting the activity of carbohydrate-hydrolyzing enzymes like α -amylase and α -glucosidase within the digestive system.^[1-3] Especially, drugs that block α -glucosidase and pancreatic α -amylase are used to treat type-2 diabetes (T2D). Examples of these drugs are Acarbose and Miglitol. It's crucial to remember that these medications might cause lactic acidosis, liver problems, hypoglycemia, and gastrointestinal issues at larger dosages. As a result, the demand for novel anti-diabetic medications with improved safety profiles is rising.

Nowadays, drug discovery relies heavily on *in silico* studies in addition to experimental methods. These computational tools make it possible to estimate binding affinities, identify chemical interactions, and examine relationships between structure and activity. The rational design and optimization of treatment options is made possible by the information provided by molecular docking and simulation studies regarding the binding mechanisms of potential inhibitors to target enzymes. Furthermore, by guiding synthetic efforts, identifying promising candidates for biological examination, and saving time and resources, *in silico* approaches improve experimental research.⁴

Organophosphorus compounds diverse variety of chemical, biological, and physical properties⁵⁻⁸ have made them extremely important in synthetic organic chemistry, agriculture, industry, and medicine. Of particular interest are α -aminophosphonates (α -Aps), a useful class of bioactive compounds that resemble active peptide transition states and have properties similar to those of natural amino acids.⁹ α -Aps possess broad range of applications in the field of industry¹⁰, biology¹¹, and medicine.^{12,13} They are useful compounds as anti-cancer agents¹⁴, antitumor reagents^{15,16}, anti-inflammatory^{17,18}, antibiotics^{19,20}, herbicides²¹, fungicides²², bactericides²³, enzyme inhibitors²⁴, plant growth regulators²⁵, anti-oxidants²⁶, protease inhibitors²⁷, metal corrosion preventor²⁸, antiviral agents²⁹, and anti-diabetic agents.^{30,31} A number of α -Aps with heterocyclic moieties have been synthesized recently and have shown significant biological activity.³²⁻³⁵ It has been discovered that adding heterocyclic structures to α -Aps greatly increases their bioactivity. The Kabachnik-Fields (K-F) reaction, which entails the nucleophilic addition of phosphites to imines, has been found to be a very effective way among the other synthetic techniques created for generating α -Aps.³⁶

Metal oxide nanoparticles have received a lot of interest as catalysts because of their high catalytic activity, environmental friendliness, ease of use, non-toxicity, and recyclability.³⁷ Zinc oxide (ZnO) is one of the most explored materials in this category. Recent literature highlights the growing interest in nano-ZnO as a heterogeneous catalyst, owing to its cost-effectiveness, low toxicity, large surface area, and environmental benefits.³⁸ Several studies have revealed that its ecologically benign features make it a promising catalyst for diverse organic reactions.³⁹⁻⁴³ Moreover, the adoption of solvent-free and environmentally benign reaction conditions aligns with the principles of green chemistry, making this approach more sustainable compared to traditional methods. Numerous studies have underscored the efficacy of nano-ZnO as a catalyst across different synthetic pathways for phosphonate synthesis.⁴⁴⁻⁴⁷

The use of microwave (MW) irradiation offers a novel way to energize reaction combinations. This method involves directly transferring energy to substrate molecules, which results in an enhanced reaction rate due to rapid kinetic excitation of molecules, pure product formation, higher yields, operational simplicity, and the potential for effective synthesis of heterocyclic bioactive compounds.^{48,49}

In disciplines including medicine, drug development, agrochemicals, dyes, photochemistry, and combinatorial chemistry, heterocyclic ring-containing compounds have attracted a lot of interest.^{50,51} Recent studies have demonstrated that organophosphorus compounds modified with heterocyclic groups can function as strong α -amylase and α -glucosidase inhibitors, giving them intriguing options for the treatment of diabetes.⁵²⁻⁵⁵ Patients with type 2 diabetes mellitus (T2DM) are frequently treated for a

variety of diabetic problems using thiazolidinediones (TZDs), a class of heterocyclic chemicals having a wide range of biological properties.⁵⁶⁻⁶² Our most recent investigation demonstrated that TZD-containing organophosphorus compounds may be useful α -amylase and α -glucosidase inhibitors for the treatment of diabetes.⁶³⁻⁷¹

This study aims to develop a new MW-assisted synthesis method for α -aminophosphonates⁷²⁻⁷⁵ utilizing a nano ZnO catalyst and evaluate its inhibitory effect on α -amylase. The study will also conduct *in vitro* studies to explore the synthesized compounds' potential anti-diabetic properties. Molecular docking research will study how these medicines attach to the active sites of α -amylase and α -glucosidase, providing insight into their inhibitory actions. This study aims to develop safer and more effective medicinal compounds for diabetes treatment by combining *in silico* analysis, synthetic chemistry, and biological evaluation.

2. Experimental

2.1. Procedures

2.1.1. Preparation of 2,4-thiazolidinedione (2)⁷⁶

In a reaction vessel, a solution of chloroacetic acid (4.73 g, 0.05 mol) (2) in 20 mL of water was mixed with a solution of thiourea (3.81 g, 0.05 mol) (1) in 20 mL of water (please write the temperature). After 15 minutes of stirring, a white precipitate formed as the mixture cooled. A dropping funnel was then used to progressively add 5 mL of concentrated hydrochloric acid, and the reaction was refluxed for 10 to 15 hours at about 105 °C. White crystals in the shape of needles developed after cooling. After being washed with water and dried, any remaining hydrochloric acid was eliminated. Recrystallization from ethyl alcohol produced the pure product, 2,4-thiazolidinedione (3), which has a melting point between 122 and 124 °C.

2.1.2. Synthesis of (E)-4-((2,4-dioxothiazolidin-5-ylidene)methyl)benzaldehyde (5)⁷⁷

Terephthalaldehyde (4.9 mL, 0.05 mol) (4) and 2,4-thiazolidinedione (5.85 g, 0.05 mol) (3) were mixed in 20 mL of toluene with piperidine as a catalytic agent. The reaction was refluxed at 110°C for about 4.5 hours and then allowed to cool to room temperature. The reaction's progress was monitored using thin-layer chromatography (TLC) with an eluent system of ethyl acetate and n-hexane in a 4:6 ratio. Once the reaction was completed, as checked by TLC, the reaction mixture was filtered, precipitate was washed to get (E)-4-((2,4-dioxothiazolidin-5-ylidene)methyl)benzaldehyde (5). Solid; yield, 90%; melting point: 228-230 °C

δ_{H} (DMSO-*d*₆): 11.25 (s, 1H, Imide-H), 10.24 (s, 1H, -C(O)-H), 7.92 (d, 2H, *J*=7.6 Hz, Ar-H), 7.65 (s, 1H, =C-H), 7.48 (d, 2H, *J*=7.6 Hz, Ar-H); δ_{C} (DMSO-*d*₆): 135.4 (C-1), 128.3 (C-2 & C-6), 143.4 (C-4), 129.1 (C-3 & C-5), 144.8 (C-7), 116.4 (C-8), 168.4 (C-9), 167.4 (C-10), 189.1 (C-11).

2.1.3. Synthesis of New Phosphonates, 8a-j Using Conventional Method

In a round-bottomed flask, to the mixture of (E)-4-((2,4-dioxothiazolidin-5-ylidene)methyl)benzaldehyde (0.14g, 0.05 mol) (5) and aniline (6a) (4.57 mL, 0.05 mol) in THF (20 mL); diethyl phosphite (7) (6.4 mL, 0.05 mol) was added drop wise with thorough stirring for 5 minutes at room temperature. The commercially available nano-ZnO (nanopowder, <100 nm particle size) (10 mol%) was added to this mixture, which was then heated to 70 °C and stirred for 3 h. TLC was used to monitor the reaction's progress using ethyl acetate: n-hexane (2:3). The reaction mixture was cooled to room temperature after the reaction was completed. DCM (15 mL) was added to the reaction content and stirred for 10 min. The catalyst, nano-ZnO was removed by filtering as residue, cleaned with DCM (2 x 10mL), and dried under vacuum at 100 °C for use in subsequent investigations. To get the crude product, the organic layer was washed with 15 mL of water, dried over anhydrous Na₂SO₄, and concentrated under vacuum at 50 °C. By utilizing column chromatography and ethyl acetate: n-hexane (3:7) as the eluent, the

Synthesis of α -aminophosphonates

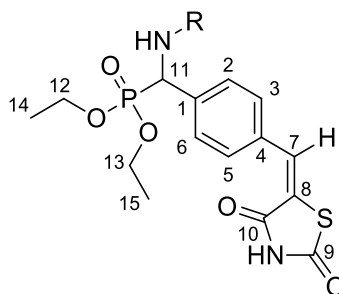
pure (E)-diethyl ((4-((2,4-dioxothiazolidin-5-ylidene)methyl)phenyl)(phenylamino)methyl)phosphonate (**8a**) was prepared. The remaining compounds **8b-j** were prepared using the same method.

2.1.4. Synthesis of Phosphonates (**8a-j**) Using Microwave Irradiation Method

A flat-bottomed flask was filled with a solution of (E)-4-((2,4-dioxothiazolidin-5-ylidene)methyl) benzaldehyde (0.14 g, 0.05 mol) (**5**), aniline (**6a**) (4.57 mL, 0.05 mol), and diethyl phosphite (**7**) (6.4 mL, 0.05 mol). Nano-ZnO (5 mol%) was then added, and the reaction mixture was microwave irradiated at 400W with a Catalyst microwave reactor-SSMW1 for 10 minutes at room temperature in solvent-free conditions. The reaction was tracked using thin-layer chromatography (TLC) with an eluent system of ethyl acetate and *n*-hexane (2:3). TLC revealed that the reaction was complete, therefore the liquid was allowed to cool to room temperature. To the reaction mixture, add 15 mL of dichloromethane (DCM) and stir for 10 minutes. The nano-ZnO catalyst was filtered, washed with DCM (2 \times 10 mL), and dried under vacuum at 100 °C before reuse. The organic layer was washed with 15 mL of water, dried over anhydrous Na₂SO₄, and concentrated under vacuum at 50 °C to provide the crude product. Purification was carried out using column chromatography with ethyl acetate and *n*-hexane (3:7) as the eluent, producing pure (E)-diethyl phosphonate (**8a**). The remaining compounds (**8b-j**) were synthesized following the same approach.

2.2. Characterization of Title Compound **8a-j**

General structure of compound **8a-j**



(E)-diethyl ((4-((2,4-dioxothiazolidin-5-ylidene)methyl)phenyl)(phenylamino)methyl)phosphonate (**8a**): solid. M.P. 151-157 °C. Yield: 96%. δ_{H} (DMSO-*d*₆): 11.60 (s, 1H, Imide-H), 7.65 (s, 1H, =C-H), 7.61 (d, $J=7.2$ Hz, 2H, Ar-H), 7.38 (t, $J=7.6$ Hz, 2H, Ar-H), 7.26 (d, $J=7.2$ Hz, 2H, Ar-H), 7.03 (d, $J=6.8$ Hz, 2H, Ar-H), 6.86 (t, $J=7.2$ Hz, 1H, Ar-H), 5.25 (s, 1H, -NH), 4.78 (d, $J=20.0$ Hz, 1H, P-CH), 4.25 (m, 2H, -O-CH₂CH₃), 4.07 (m, 1H, -O-CH₂CH₃), 3.91 (m, 1H, -O-CH₂CH₃), 1.23 (t, $J=6.8$ Hz, 3H, -O-CH₂CH₃), 1.12 (t, $J=6.8$ Hz, 3H, -O-CH₂CH₃); δ_{C} (DMSO-*d*₆): 168.73 (C-9), 167.05 (C-10), 148.47 (C-1), 144.35 (C-7), 136.75 (C-1), 135.17 (C-4), 131.25 (C-3', C-5), 128.94 (C-3, C-5), 127.54 (C-2, C-6), 121.62 (C-4), 115.41 (C-8), 114.24 (C-2', C-6'), 67.51 (d, $J=100.6$ Hz, C-11), 63.11 (d, $J=5.7$ Hz, C-12), 62.31 (d, $J=5.0$ Hz, C-13), 13.64 (d, $J=5.0$ Hz, C-14), 12.65 (d, $J=10.5$ Hz, C-15); δ_{P} (DMSO-*d*₆): 15.1 ppm; IR (KBr) (ν_{max} cm⁻¹): 3330, 3125 (NH), 1733 (C=O), 1206 (P=O), 1017 (P-O-C_{alip}); LCMS (m/z , %): 447 (M+H⁺, 100); Anal. Calcd. for C₂₁H₂₃N₂O₅PS; calcd: C, 56.49; H, 5.19; N, 6.27%; found: C, 56.60; H, 5.10; N, 6.36%.

2.3. In silico ADME Analysis

All of the proposed compounds' physicochemical properties, lipophilicity, water solubility, pharmacokinetics/ADME, drug-likeness, and medicinal chemistry characteristics were predicted computationally using the Swiss ADME tool developed by the Swiss Institute of Bioinformatics (<http://www.sib.swiss>).

2.4. *In silico* Molecular Docking Studies

Using *in silico* molecular docking, the binding mechanism of **8a-j** with the targeted enzyme, pancreatic α -amylase (PDB ID: 3IJ8) and α -glucosidase (PDB ID: 3WY1) was examined. The crystal structure of the enzymes was obtained using the RCSB, Protein Data Bank (PDB ID: 3IJ8 and PDB ID: 3WY1). To improve efficiency, water molecules, heteroatoms, and co-factors were eliminated from the structure. Charges, hydrogen bonds, and missing atoms were added. To execute molecular docking, the 1-Click docking online server program (<https://mcutle.com>) was used with the default binding site centres X: 7.2178, Y: 16.2957, and Z: 42.1167 and X: -10.6207, Y: -15.320, and Z: 17.3104 respectively for docking studies on α -amylase and α -glucosidase enzymes. The discovery studio visualizer V16.1.0.15350 was used to explore the process of docking ligands with proteins and their interactions.

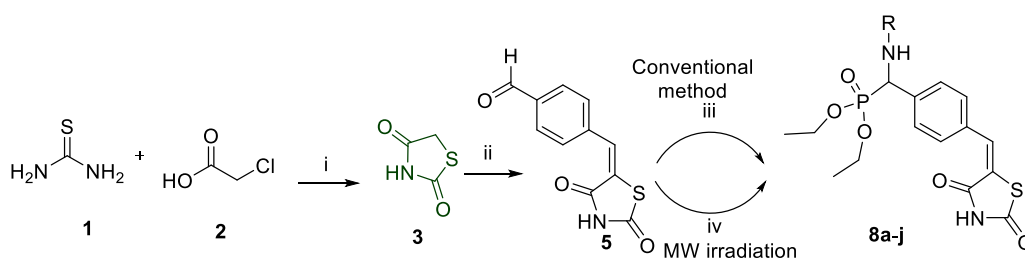
2.5. α -Amylase Inhibitory Activity

The novel synthesised compounds' α -amylase inhibitory activity was tested using established methods with minor modifications. (For a complete procedure, see Supplemental Materials.) The half-maximal inhibitory concentration (IC_{50}) is an excellent indicator of a drug's efficacy. It is a measure of antagonist drug potency in pharmacological research because it shows the amount of drug required to block a biological process by half. The IC_{50} values in this investigation were derived by graphing concentration (X-axis) versus percent inhibitory action (Y-axis). Using the linear ($y=mx+c$) equation on this graph for $y=50$, the value of the x point is transformed into the IC_{50} value. A one-way ANOVA test was performed to assess the overall significance of differences among the compounds, followed by Tukey's HSD post hoc test for pairwise comparisons.

3. Results and Discussion

3.1. Chemistry

In this study, we created several novel phosphonates (**8a-j**) with α -amylase inhibitory action that was anticipated by *in silico* molecular docking studies and ADMET analysis. The compounds with a high docking score were subsequently synthesized with high yields (93-97%) utilising MW irradiation in a solvent-free nano-ZnO catalyzed method. Scheme 1 depicts the synthesis approach for phosphonates (**8a-j**). The detailed mechanism for the synthesis was made available in the supplemental materials as Figure S1.

Synthesis of α -aminophosphonates

i). H₂O, r.t. ii) terephthalaldehyde (**4**), piperidine, toluene, r.t.; iii) Catalyst, THF, R-NH₂ (**6a-j**), diethyl phosphite (**7**); iv) US, R-NH₂ (**6a-j**), diethyl phosphite (**7**)

Compd	8a	8b	8c	8d	8e
R					
Compd	8f	8g	8h	8i	8j
R					

Scheme 1. MW facilitated synthesis of phosphonates **8a-j** catalyzed by nano-ZnO

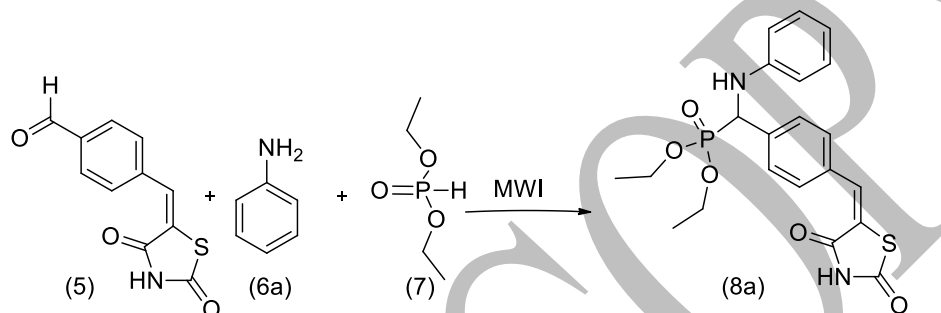
Table 1. Preparation of compound **8a** under various conditions^a

Entry	Catalyst (mol%)	Solvent	Temp. (°C)	Time	Yield ^b (%)
1	-----	THF	r.t.	24 h	42
2	Et ₃ N (1.2 eq.)	THF	r.t.	12 h	50
3	FeCl ₃ (5)	THF	r.t.	12 h	69
4	AlCl ₃ (5)	THF	r.t.	12 h	72
5	LaCl ₃ (5)	THF	r.t.	12 h	74
6	MnO ₂ (5)	THF	r.t.	12 h	70
7	CuCl ₂ (5)	THF	r.t.	12 h	72
8	NiBr ₂ (5)	THF	r.t.	12 h	77
9	TiO ₂ (5)	THF	r.t.	12 h	76
10	ZnCl ₂ (5)	THF	r.t.	8 h	78
11	ZnBr ₂ (5)	THF	r.t.	8 h	79
12	ZnO (5)	THF	r.t.	6 h	80
13	Nano-ZnO (5)	THF	r.t.	2 h	88
14	Nano-ZnO (5)	DMF	r.t.	2 h	86
15	Nano-ZnO (5)	1,4-dioxane	r.t.	2 h	87
16	Nano-ZnO (5)	methanol	r.t.	2 h	87
17	Nano-ZnO (5)	DCM	r.t.	2 h	88
18	Nano-ZnO (5)	Toluene	45	2 h	86
19	Nano-ZnO (5)	Solvent-free	Room temp.	2 h	92
20	Nano-ZnO (5)	Solvent-free, MWI	Room temp.	9 minutes	96

^aReaction between (E)-4-((2,4-dioxothiazolidin-5-ylidene) methyl) benzaldehyde (**5**), aniline (**6a**) and diethyl phosphite (**7**) was selected as model to optimize conditions of reaction

^bIsolated yield

Initially, a model reaction using benzaldehyde **5** (0.14g, 0.05 mol), aniline (**6a**) (4.57 mL, 0.05 mol) and diethyl phosphite (**7**) (6.4 mL, 0.05 mol) was performed. At the start of the study, the reaction was carried out at reflux temperature (r.t.) using tetrahydrofuran (THF) as the solvent and no catalyst. After 24 hours, the product, (E)-diethyl ((4-((2,4-dioxothiazolidin-5-ylidene) methyl) phenyl) (phenylamino)methyl) phosphonate (**8a**), was obtained with a low yield (42%) (Table 1, entry 1). The reaction was then carried out in presence of triethylamine (1.2 equivalents). We obtained a yield of 50% (Table 1, entry 2). The reaction was then carried out with the aid of a catalyst. In search of an efficient catalyst, the model reaction was carried out utilizing catalysts (5 mol%) such as FeCl₃, AlCl₃, LaCl₃, MnO₂, CuCl₂, NiBr₂, TiO₂, ZnCl₂, ZnBr₂ and ZnO (Entries 3-12 in Table 1). The yield of product **8a** increased from 69-80% after 6-12 hours, indicating that the catalyst plays an essential role in this process.



Scheme 2. Synthesis of compound **8a**

Based on a recent survey of the literature, nano-ZnO, as a heterogeneous catalyst, has garnered significant interest owing to its affordability, lack of toxicity, and positive ecological impact.⁷⁸ Given its numerous benefits, researchers have explored its potential as a potent catalyst for a wide range of organic reactions.⁷⁹ As a result, the compound **8a** was synthesized in the model reaction utilizing nano-ZnO (5 mol%). When THF was used as the solvent, a good yield (88%) of compound **8a** (Table 1, entry 13) was obtained in 2 hours. To examine the effect of solvent on the process, various solvents such as DMF, 1,4-dioxane, methanol, Dichloromethane (DCM), and Toluene were utilized. In this study, there was no discernible yield of the products (86-88%) (Table 1, entries 14-18). We then tried this procedure without a solvent. In this scenario, a high product yield (92%) was achieved in 1 hour (Table 1, entry 19). To optimize the reaction conditions and decrease the reaction time, the reaction mixture was MW irradiated without solvent utilizing nano-ZnO (5 mol%) as a catalyst to increase the yield and reaction conditions. We were able to obtain a greater yield (96%) of **8a** in this condition in just 9 minutes (Table 1, entry 20).

Table 2. The consequence of the amount of the catalyst, Nano-ZnO to promote the K-F reaction^a

Entry	Amount of Catalyst (mol%)	Time (min)	Yield ^b (%)
1	1	9	86
2	2.5	9	93
3	5	9	94
4	7.5	9	96
5	10	9	96

^aReaction between (E)-4-((2,4-dioxothiazolidin-5-ylidene) methyl) benzaldehyde (**5**), aniline (**6a**) and diethyl phosphite (**7**) was selected as model to optimize conditions of reaction

^bIsolated yield

By changing the catalyst concentration from 1 to 10 mol% under microwave (MW) irradiation and solvent-free conditions, the impact of catalyst (Nano-ZnO) loading on the Kabachnik–Fields (K-F) reaction was methodically investigated (Table 2, Entry 1–5). According to the study, a catalyst loading of 1 mol% (Entry 1) produced a reasonable yield of 86%, however an increase to 2.5 mol% (Entry 2) greatly

Synthesis of α -aminophosphonates

increased the yield to 93%. It was found that 5 mol% of catalyst produced 94% of the desired result (Entry 3). A slightly greater yield of 96% was obtained by increasing the catalyst loading to 7.5 mol% (Entry 4). This yield did not change at 10 mol% (Entry 5), suggesting that more catalyst did not improve the reaction efficiency. These results led to the selection of 7.5 mol% of Nano-ZnO for additional research, ensuring a high yield while preserving catalytic efficiency.

In the model reaction, the reusability of Nano-ZnO (7.5 mol%) was assessed over six successive cycles with the same reaction conditions (Table 3, Entry 1–6). Following each reaction, the product was separated, and the leftover catalyst was washed with chloroform to get rid of any residues that had been adsorbed on the surface before being used again. The catalyst's initial activity was high, resulting in a 95% yield in the first run (Entry 1). The yield steadily declined in the next cycles, reaching 93%, 91%, and 88% in the second, third, and fourth runs, respectively (Entries 2-4). The yield decreased more sharply to 82% and 81% in the fifth and sixth cycles (Entries 5-6), indicating a gradual reduction in catalytic efficiency brought on by possible active site leaching, aggregation, or deactivation. These findings show that Nano-ZnO is a sustainable and promising heterogeneous catalyst for phosphonate synthesis in environmentally friendly and solvent-free circumstances due to its effective catalytic activity and strong reusability.

Table 3. Nano-ZnO (7.5 mol%) catalyst reusability for the synthesis of compound **8a**^a

Entry	Nano-ZnO (7.5 mol%)	Time (min.)	Yield ^b (%)
1	1 st run	9	95
2	2 nd run	9	93
3	3 rd run	9	91
4	4 th run	9	88
5	5 th run	9	82
6	6 th run	9	81

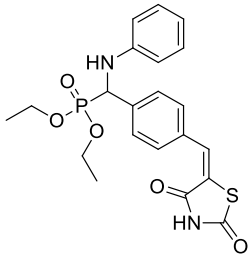
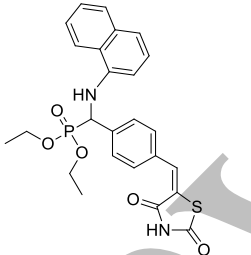
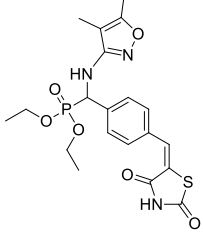
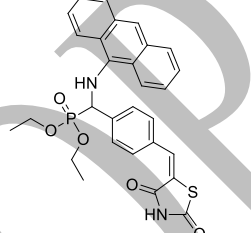
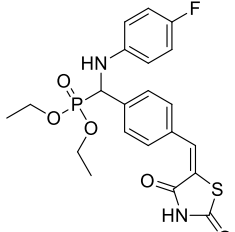
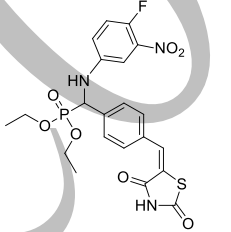
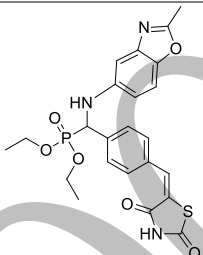
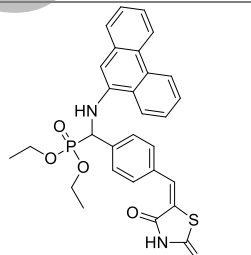
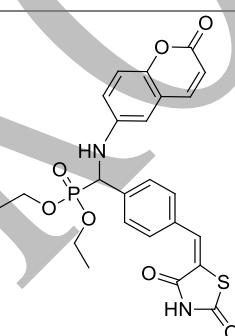
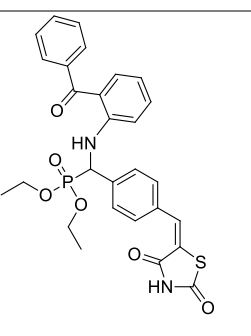
^aReaction between (E)-4-((2,4-dioxothiazolidin-5-ylidene)methyl)benzaldehyde (**5**), aniline (**6a**) and diethyl phosphite (**7**) was selected as model to optimize reaction conditions

^bIsolated yield

3.2. General Discussion of Spectral Data for Compounds **8a-j**

NMR (¹H, ¹³C, ³¹P), mass, IR spectroscopy, and elemental investigations, were employed to better understand the structures of the newly synthesized compounds **8a-j**. All compounds have a single phosphorus resonance in ³¹P NMR spectra, with a δ 22.7-15.1 ppm range that is consistent with phosphonate esters.⁸⁰⁻⁸² Small upfield or downfield shifts are caused by substituents on the aromatic ring. Compounds **8a-j**'s proton NMR spectra show multiplets of aromatic protons in the range δ 8.84-6.63 ppm, which are caused by different substituents. A singlet of the imide (-NH) proton at δ 11.67-11.65 ppm confirms the presence of the thiazolidinone moiety. The vinylic (-CH=) proton is found in the δ 7.68-7.65 ppm range as a singlet. Depending on the coupling, aliphatic protons from ethoxy groups usually appear as triplets or quartets and resonate between δ 4.30-1.12 ppm. The detection of signals in the δ 168.73-167.05 ppm range, which correspond to carbonyl (C=O) carbons, validates the thiazolidinone moiety's functioning. In accordance with the anticipated shifts for benzyl and isoxazole rings, the aromatic carbons resonate between δ 153.35 and 103.66 ppm, depending on the type of substituents on the aromatic ring. The presence of the conjugated benzylidene (-CH=) carbon at δ 144.35 ppm indicates that it is electron-deficient. The presence of the phosphonate moiety is confirmed by the phosphonate (-P-CH) carbon, which is detected at the δ 67.45 ppm area and shows a strong coupling ($J = 101.5$ Hz) with phosphorus. The aliphatic carbons of the ethoxy (-OCH₂CH₃) groups resonate between δ 63.12-12.65 ppm, depending on how close they are to the phosphorus atom. The effective synthesis of the phosphonate derivatives is confirmed by these chemical shift assignments; some variations among related compounds are anticipated as a result of electronic influences and substituent effects. The IR spectra of infrared spectroscopy (IR) show distinctive stretching bands for important functional groups.

Table 4. *MW mediated nano-ZnO catalyzed synthesis of phosphonates (**8a-j**)^a

Compound	Structure	Time (min)	Yield ^b (%)	Compd	Compd	Time (min)	Yield ^b (%)
8a		10	96	8f		18	96
8b		12	95	8g		12	97
8c		12	93	8h		15	93
8d		10	95	8i		18	95
8e		10	94	8j		15	97

^aReaction between (E)-4-((2,4-dioxothiazolidin-5-ylidene)methyl)benzaldehyde (**5**), aniline (**6a-j**) and diethyl phosphite (**7**) was selected as model to optimize reaction conditions. *MW irradiated with 400W using Catalyst microwave reactor-SSMW1 (Frequency: 2.45 GHz) for 10 minutes at ambient temperature

^bIsolated yield

The presence of the amide group is confirmed by the N-H stretch at 3310-3120 cm⁻¹. The carbonyl groups are indicated by the C=O stretch about 1747-1721 cm⁻¹. The phosphonate ester group is validated

Synthesis of α -aminophosphonates

by the P=O stretch at 1223-1210 cm^{-1} . The structures of the compounds are confirmed by the molecular ion peaks ($[\text{M}+\text{H}]^+$) in mass spectrometry (LCMS), which match the estimated molecular weights of the compounds.

The Supplementary Materials encompassed standard spectra (^1H , ^{31}P , ^{13}C NMR, IR, Mass spectra and CHN analysis) for compounds **8a** as representative of compounds **8a-j**.

3.3. Pharmacology

3.3.1. ADME Analysis *in Silico*,

In Silico ADME analysis, utilizing computational models, predicts drug candidates' pharmacokinetic properties, offering multiple advantages in drug discovery. It enables early screening of compound libraries, aiding in the identification of promising candidates and reducing the need for laborious experimental assays.⁸³ Additionally, it accurately forecasts oral bioavailability by assessing solubility, permeability, and metabolic stability, crucial for optimizing drug absorption.⁸⁴ Moreover, it models tissue distribution, providing insights into drug spatial distribution and aiding in designing compounds with enhanced efficacy.⁸⁵ Overall, *in silico* ADME analysis streamlines decision-making, cuts development costs, and enhances the likelihood of success in clinical trials.

The ADME bounds of the proposed molecules were verified using SwissADME, which might be downloaded from the website <http://www.swissadme.ch>. The estimate was based on the physicochemical and structural advantages of the moieties. Table S1 shows the physicochemical properties of the molecules **8a-j** (See Supplemental materials for details). All evaluated compounds **8a-j**, as well as acarbose as a reference drug, do not violate the Lipinski rule because their values are within the normal range, and these metrics demonstrated a reasonable bioavailability score when compared to acarbose, as well as respectable agreement with all appropriate criteria for molecules **8a-j**. Table S2 inclines the ADME parameters for the newly mass-produced compounds (See Supplemental materials for details). All the molecules were shown to have a low gastrointestinal absorption (GI). The BOILED-Egg model's results indicate evaluations for both human stomach absorption and passive blood-brain barrier (BBB) permeability (HIA).⁸⁶ Figures S7 and S8 display the boiled egg representation, along with bio radar images of molecules **8a-j** (See Supplemental materials for details). No molecules are projected to undergo passive absorption within the gastrointestinal tract and passively traverse the BBB. Assessing the propensity of compounds to act as substrates or non-substrates for the permeability glycoprotein (PGP), particularly in scenarios involving movement from the gastrointestinal wall to the lumen, aids in the evaluation of active efflux across biological membranes.⁸⁷ Importantly, all screened molecules except **8b**, are predicted not to be effluxed from the central nervous system by p-glycoprotein (PGP - indicated by red dots). In the context of a pharmacokinetic investigation, it is imperative to predict the potential for significant drug interactions arising from the inhibition of cytochrome enzymes (CYPs) like CYP2C19, CYP1A2, CYP2C9, CYP3A4, and CYP2D6 and to identify which specific isoenzymes would be affected.^{88,89} All tested substances were projected to inhibit CYP2C9 and CYP3A4. No molecules are found to be the inhibitors of CYP1A2. Substances **8a**, **8b**, **8c**, **8d**, **8f** and **8h** were identified as inhibitors of CYP2C19, while, except **8b**, **8c** and **8h**, the rest of the compounds were expected to have no inhibitory effects on CYP2D6. Notably, none of these isoenzymes exhibited inhibitory effects on the reference drug. Additionally, a multiple linear regression model was employed to estimate the skin permeability coefficient (Kp). Potts and Guy⁹⁰ observed a linear correlation between molecule size, Kp, and lipophilicity ($R^2=0.67$). Among the compounds in question, **8a**, **8b**, **8c**, **8e** and **8h** demonstrated the most substantial negative logarithmic Kp values, indicative of lower skin permeability. Conversely, the reference medication displayed the lowest permeability to skin and the uppermost log Kp value (-16.29) among all the compounds examined.

By assessing drug-likeness variables, researchers can qualitatively evaluate whether a compound possesses the key properties needed to become a successful and highly bioavailable oral medication. Therefore, we applied a set of 5 rules⁹¹⁻⁹⁵ to assess the drug-likeness and oral bioavailability of the synthesized compounds. With only a few exceptions, all the molecules adhered to these five principles. In Table 5, you'll find properties of compounds **8a-j** related to drug similarity. Remarkably, except for

acarbose (with a score of 0.17), all the compounds examined scored a robust 0.55 on bioavailability, indicating their strong suitability. The absence of pan assay interference compounds (PAINS) cautions except in **8j** suggests that the lead molecules exhibit a favorable pharmacokinetic profile. Most of these compounds displayed favorable pharmacokinetic, physicochemical, and drug-like attributes when equated to the reference drug.

Table 5. Drug likeness properties of compounds **8a-j**

Compound	Lipinski violations	Ghose violations	Veber violations	Egan violations	Muegge violations	B.S	PAINS alerts	S.A.
8a	0	0	0	0	0	0.55	0	4.6
8b	0	0	1	1	1	0.55	0	4.77
8c	0	0	0	0	0	0.55	0	4.56
8d	1	2	1	1	1	0.55	0	4.77
8e	1	2	1	1	1	0.55	0	4.9
8f	0	2	0	0	1	0.55	0	4.83
8g	1	3	0	1	1	0.55	0	5.06
8h	1	2	1	1	1	0.55	0	4.69
8i	1	3	0	1	1	0.55	0	5.06
8j	1	3	2	1	1	0.55	1	5.04
Acarbose	3	4	1	1	5	0.17	0	7.25

Std*: Acarbose; B.S.: S.A.: Synthetic Accessibility; Bioavailability Score

3.3.2. In silico Molecular Docking Study on α -Amylase Enzyme

We utilized the 1-click docking online server application⁹⁶, known for its compatibility with the AutoDock Vina docking algorithm, to perform in silico testing of all synthesized compounds against the pancreatic α -amylase enzyme. The screening results revealed notable improvements in binding energies equated to the reference medication, acarbose (-8.2 kcal/mol). Specifically, all compounds exhibited superior or virtually equivalent binding energies, ranging from -8.9 to -8.0 kcal/mol. Detailed information regarding these binding energies and the consistent complex bonding postures can be found in Table S3 of the supplemental materials.

Table 6. Molecular Docking Interactions of Synthesized Compounds with α -Amylase

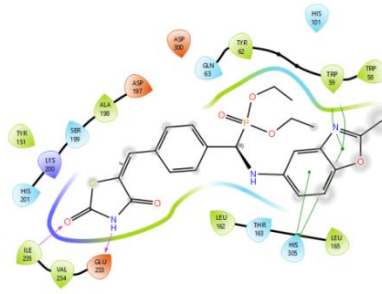
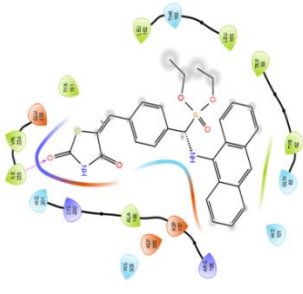
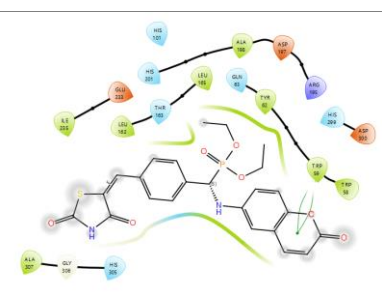
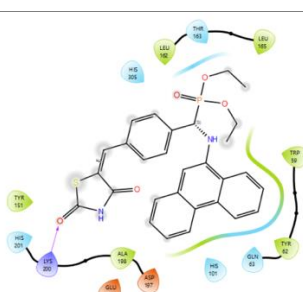
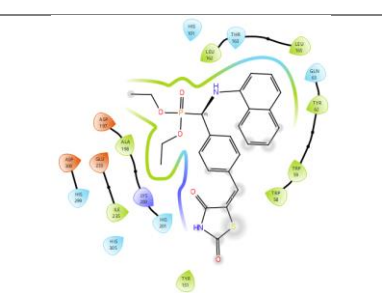
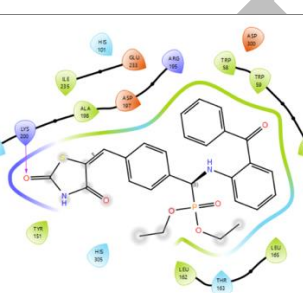
Compound	Hydrogen Bonding	π - π Stacking	Hydrophobic Interactions
8i	LYS200	None	LEU165, LEU162, TRP59, TYR62, ALA198, TYR151
8d	ILE235, GLU233	HIS305, TRP59	LEU165, LEU162, VAL234, ILE235, TYR151, ALA196, TYR62, TRP59, TRP58
8e	NONE	TRP59	ILE235, ALA198, LEU162, LEU165, TYR62, TRP59, TRP58, ALA307
8g	ILE235	None	ILE235, VAL234, TYR151, LEU162, LEU165, TRP59, TYR62, ALA198
8j	LYS200	None	ILE235, TRP58, TYR62, TRP59, LEU165, LEU162, TYR151, ALA198
8f	ILE235	None	ILE235, VAL234, TYR151, LEU162, LEU165, TRP59, TYR62, ALA198

The compounds **8i** (-8.9 kcal/mol), **8g** (-8.8 kcal/mol), and **8j** (-8.6 kcal/mol) showed the best binding interactions among the investigated compounds, indicating a strong potential for enzyme inhibition. The title compounds' binding energies are arranged as follows: **8i** (-8.9 kcal/mol) > **8g** (-8.8 kcal/mol) > **8j** (-8.6 kcal/mol) > **8e** (-8.5 kcal/mol) > **8f** (8.3 kcal/mol) > **8d** (8.2 kcal/mol) > **8a** (8.1 kcal/mol) = **8b** (8.1 kcal/mol) > **8c** (8.0 kcal/mol) = **8h** (8.0 kcal/mol). To gain deeper insight into the

Synthesis of α -aminophosphonates

binding mechanism, we examined specific ligand–protein interactions, including π – π stacking, hydrogen bonding, hydrophobic contacts, and electrostatic interactions. These interactions are compiled in Table 6.

Table 7. 2D Lig Plot pictures of compounds **8d**, **8e**, **8f**, **8g**, **8i** and **8j**

Compound	2D structure	Compd	2D structure
8d		8g	
8e		8i	
8f		8j	

● Charged (negative)

● Charged (positive)

● Glycine

● Hydrophobic

● Metal

● Polar

● Unspecified residue

● Water

● Hydration site

✗ Hydration site (displaced)

⋯ Distance

→ H-bond

→ Halogen bond

— Metal coordination

— Pi-Pi stacking

— Pi-cation

— Salt bridge

○ Solvent exposure

The molecular docking investigation of produced drugs against α -glucosidase identifies critical interactions that lead to inhibitory activity. Hydrogen bonding was most prevalent in compounds **8i**, **8d**, **8g**, **8j**, and **8f**, with Ile235 and Lys200 being the most commonly implicated residues. These interactions are expected to increase the stability of ligand binding inside the active site. In **8d** and **8e**, π – π stacking interactions were observed, with Trp59, His305, and Phe residues contributing significantly to binding affinity. Hydrophobic interactions were found throughout all compounds, with residues Leu165, Leu162, Trp59, Tyr62, Ala198, and Tyr151 consistently contributing to ligand stabilization.

Among all studied compounds, **8d** demonstrated the most extensive interactions, participating in hydrogen bonding, π – π stacking, and numerous hydrophobic contacts, indicating a considerable binding affinity. Compounds with several interaction types, such as hydrogen bonds and π – π stacking, have higher

inhibitory potential. Therefore, **8d** and **8e** are interesting candidates for future development as α -glucosidase inhibitors.

These findings provide insight into the complex chemical interactions that contribute to the inhibitory effect of produced compounds against pancreatic α -amylase. This provides useful insights for future medication design and optimization. The 2D ligand diagrams in Table 7 provide visual representations of these binding contacts, which aids in the interpretation of the observed interactions.

3.3.3. *In silico* Molecular Docking Study on α -Glucosidase Enzyme

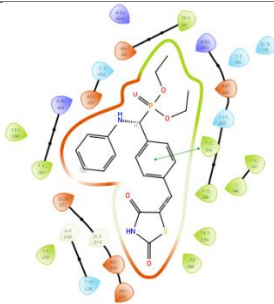
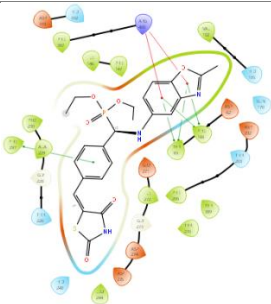
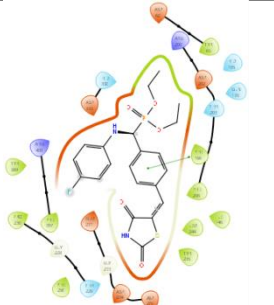
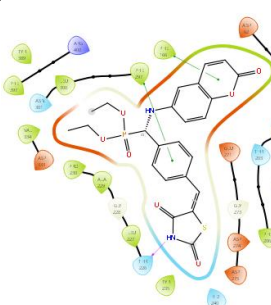
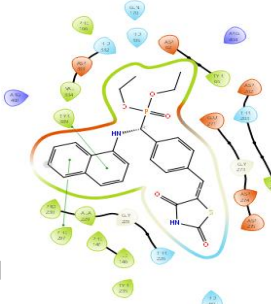
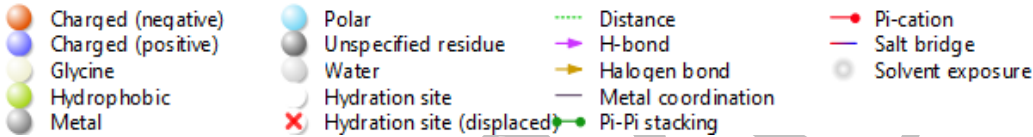
The binding potential of produced compounds with pancreatic α -glucosidase enzyme was examined through *in silico* molecular docking utilizing the 1-Click Docking web server (<http://mcule.com/apps/1-click-docking/>) and verified using the AutoDock Vina docking technique.⁹⁶ The docking data showed that all compounds had binding energies ranging from -6.4 to +1.7 kcal/mol, which were comparable to or better than those of the reference medication, acarbose. Table S4 contains detailed information on binding energies and molecular interactions (refer to supplementary materials).

Table 8. Molecular Docking Interactions of Synthesized Compounds with α -glucosidase

Compound	Hydrogen Bonding	π - π Stacking	π -Cation Interaction	Hydrophobic Interactions
8a	None	PHE166 (Phenyl group)	None	PHE397, TYR389, TYR65, PHE166, PHE206, ILE146, PHE147, TYR235, LEU244, PHE297
8c	None	PHE166 (Phenyl group)	None	TYR389, TYR65, PHE166, PHE206, LEU244, ILE146, TYR235, PHE297, PRO230, PHE397
8e	Thr226 (TZD moiety)	PHE297, PHE166 (2-oxo-2H-chromen-6-yl and Phenyl group)	None	LEU300, PHE297, PHE166, TYR65, PHE147, ILE146, LEU244, PHE206, TYR235, LEU227, ALA229, PRO230, VAL334
8d	None	PHE166, TYR65, PHE297 (2-methylbenzo[d]oxazol-5-yl and Phenyl group)	ARG400 (2-methylbenzo[d]oxazol-5-yl group)	PHE397, ILE146, PHE147, VAL102, PHE166, TYR65, ILE272, PHE206, TYR389, TYR236, ILE244, PHE297, PRO230, ALA229
8f	None	TYR389, PHE297 (2-methylbenzo[d]oxazol-5-yl and Phenyl group)	None	PHE166, TYR65, PHE206, ILE146, TYR235, PHE147, PHE297, ALA229, PRO230, TYR389, VAL334

All the screened molecules (**4a–j**) displayed effective docking interactions, with binding energies ranging from -6.4 to +1.7 kcal/mol. Among the ten compounds in this series, **8a**, **8b**, **8c**, **8d**, **8e**, **8f**, and **8j** demonstrated higher binding affinities compared to the reference drug, which had a binding energy of -2.0 kcal/mol. The binding energy of the title compounds is in the order of **8a** (-6.4 kcal/mol) > **8c** (-5.8 kcal/mol) > **8e** (-5.5 kcal/mol) > **8d** (-5.0 kcal/mol) > **8f** (4.2 kcal/mol) > **8h** (-3.2 kcal/mol) = **8b** (-3.1 kcal/mol) = **8i** (-1.1 kcal/mol) > **8j** (-0.6 kcal/mol) > **8g** (1.7 kcal/mol). We examined particular ligand-protein interactions, such as π - π stacking, hydrogen bonding, hydrophobic contacts, and π -Cation interactions, to learn more about the binding mechanism. These interactions are compiled in Table 8.

Synthesis of α -aminophosphonates**Table 9.** 2D Lig Plot pictures of compounds **8a**, **8c**, **8d**, **8e**, and **8f**

Compound	2D structure	Compd	2D structure
8a		8d	
8c		8e	
		8f	
			

Molecular docking investigation of produced drugs against α -glucosidase showed substantial interactions that contribute to their inhibitory potential. Compound **8e** exhibited hydrogen bonding, with the TZD moiety forming a connection with Thr226, indicating its function in ligand-protein complex stability. π - π stacking interactions were predominant across numerous compounds, particularly **8a**, **8c**, **8d**, **8e**, and **8f**. Phe166, Phe297, and Tyr389 played a critical role in increasing ligand binding. Compound **8d** exhibits a novel π -cation interaction with Arg400, which may contribute to its increased binding affinity. Hydrophobic interactions were widely dispersed across all investigated substances, with residues Phe166, Tyr65, Phe206, Ile146, Tyr235, and Phe297 often implicated, indicating that the enzyme's binding pocket is conserved. The compounds **8d** and **8e** showed the most extensive interactions, including hydrogen bonding, π - π stacking, and hydrophobic contacts, indicating their potential as strong α -glucosidase inhibitors. These findings provide useful insights for the rational design of new α -glucosidase inhibitors. **8d** and **8e** are interesting candidates for future optimization and drug development.

In systematic literature, 2D diagrams are used to identify the target protein's binding interactions with the ligands. Table 9 shows the 2D ligand diagrams of molecules 8a, 8c, 8d, 8e, and 8f, which indicate their binding interactions with the target enzyme.

3.3.4. *In vitro* α -amylase Inhibitory Assay

The synthesized compounds were examined *in vitro* for their ability to inhibit α -amylase using a modified version of a typical procedure.^{97,98} The enzyme α -amylase is involved in the breakdown of carbohydrates, making it a potential target for managing conditions like diabetes.

Structural Activity Relationships (SAR) analysis reveals specific structural motifs that influence inhibitory potency. Compounds bearing certain aromatic moieties demonstrated notable efficacy. For instance, compounds **8g** (IC_{50} , 99.2 \pm 0.5 μ g/mL), **8i** (IC_{50} , 101.2 \pm 0.3 μ g/mL), **8e** (IC_{50} , 102.1 \pm 0.4 μ g/mL) and **8j** (IC_{50} , 103.4 \pm 0.4 μ g/mL) containing anthracen-9-ylamino, phenanthren-9-ylamino, 2-oxo-2H-chromen-6-yl)amino and 2-benzoylphenyl)amino moieties respectively, exhibited the highest inhibitory activity, surpassing the reference compound acarbose (IC_{50} , 104.5 \pm 0.1 μ g/mL). This suggests a potential role of these aromatic systems in enhancing α -amylase inhibition. Further, SAR insights indicate that compounds **8d** (IC_{50} , 106.6 \pm 0.9 μ g/mL) with 2-methylbenzo[d]oxazol-5-yl)amino)methyl substituent, **8f** (IC_{50} , 110.6 \pm 0.8 μ g/mL) with naphthalen-1-ylamino substituents displayed comparable inhibitory effects to acarbose, although slightly less potent. Additionally, the range of IC_{50} values from 117.9 \pm 0.1 to 149.7 \pm 0.1 μ g/mL for the remaining compounds (**8a**, **8b**, **8c**, and **8h**) indicates moderate to good inhibitory activity. This variability underscores the impact of structural modifications on the efficacy of α -amylase inhibition. Figure 1 shows the IC_{50} values for all compounds. Figure S10 presumably depicts the percentage inhibition of the title compounds **8a-j**. (See Supplemental materials for details)

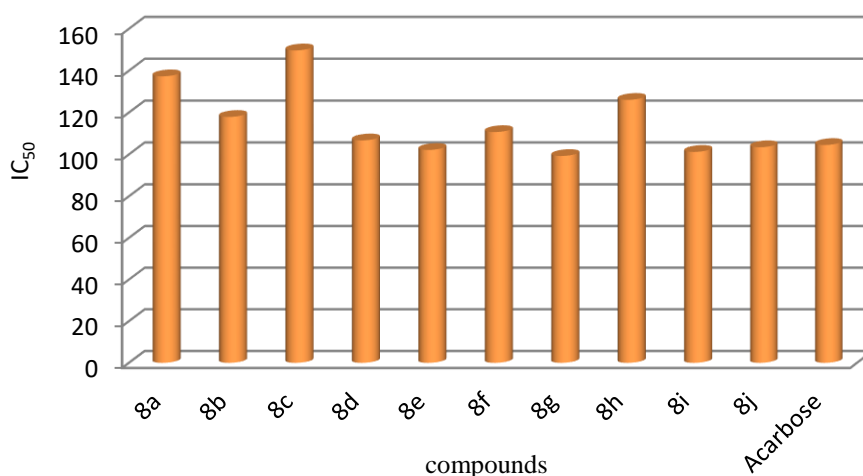


Figure 1. IC_{50} values of compounds **8a-j**

3.3.5. Statistical Analysis of α -Amylase Inhibition Assay

The IC_{50} values of compounds **8a-j** were measured in triplicate and statistically examined to assess their α -amylase inhibitory action. To determine the overall significance of the differences between the compounds, a one-way ANOVA test was conducted. For pairwise comparisons, Tukey's HSD post hoc test was then used. The ANOVA results confirmed that the compounds' inhibitory effects differed significantly, with a very significant variation among the investigated substances ($F = 66663.47$, $p = 6.89 \times 10^{-47}$). Significant differences across several compound pairs were also found using Tukey's multiple

Synthesis of α -aminophosphonates

comparison test, suggesting that some derivatives had significantly stronger or lower α -amylase inhibition than others. These variations are evident in the box plot representation of IC_{50} values (Figure 2), where compounds **8g**, **8i**, and **8e** exhibit the lowest IC_{50} values and, consequently, the maximum inhibitory activity. Compound **8c**, on the other hand, showed the highest IC_{50} value, suggesting a weaker inhibition. The promise of these compounds as α -amylase inhibitors is further supported by the fact that the reference medication Acarbose showed inhibition comparable to several developed derivatives. These results emphasize that substituent alterations have a considerable impact on inhibitory potency and highlight the structure-activity correlations (SAR) among the produced compounds. In summary, the SAR analysis elucidates the importance of specific structural features, particularly aromatic substituents, in enhancing α -amylase inhibitory activity, thereby guiding the design of more potent inhibitors for therapeutic applications.

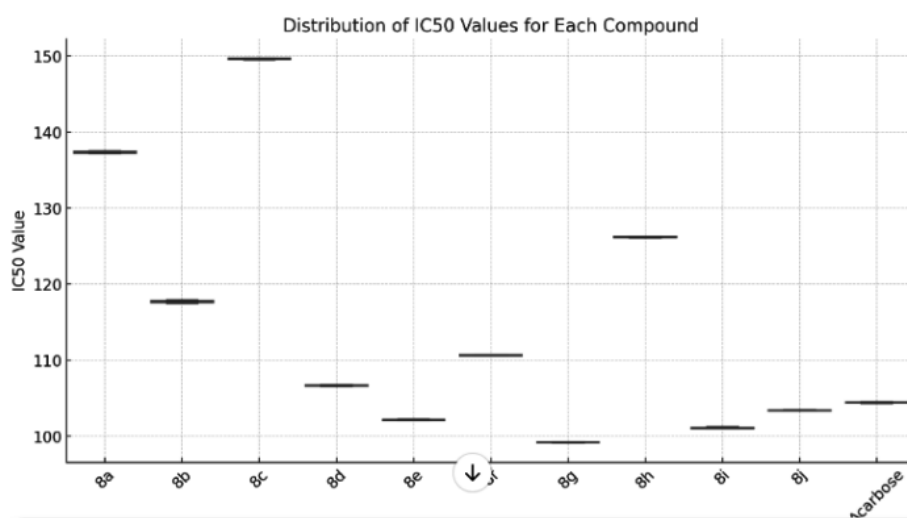


Figure 2. Box plot of IC_{50} values for α -amylase inhibition

3.3.6. *In vitro* α -glucosidase Inhibition Assay

The prepared compounds were examined *in vitro* for their aptitude to inhibit α -glucosidase using a modified version of a typical procedure.⁹⁹ At doses of 25, 50, 100, 150, 200, and 250 μ g/mL, the screening was conducted. The majority of the chemicals successfully inhibited the target enzyme. **8c** bearing with 4-fluorophenyl substituent (IC_{50} , 88.4 ± 0.7 μ g/mL), **8e** (IC_{50} , 90.0 ± 0.4 μ g/mL) bearing with 2-oxo-2H-chromen-6-yl substituent and **8d** (IC_{50} , 91.1 ± 0.9 μ g/mL) bearing with 2-methylbenzo[d]oxazol-5-yl moiety demonstrated more inhibitory efficacy than the reference medication, Acarbose (IC_{50} , 93.1 ± 0.8 μ g/mL). The leftover compounds exhibited good to moderate inhibition on the enzyme with IC_{50} ranging 94.5 \pm 0.9 to 141.4 \pm 0.7 μ g/mL. Figure 3 shows the IC_{50} values for all compounds. Figure S11 presumably depicts the percentage inhibition of the title compounds **8a-j**. (See Supplemental materials for details)

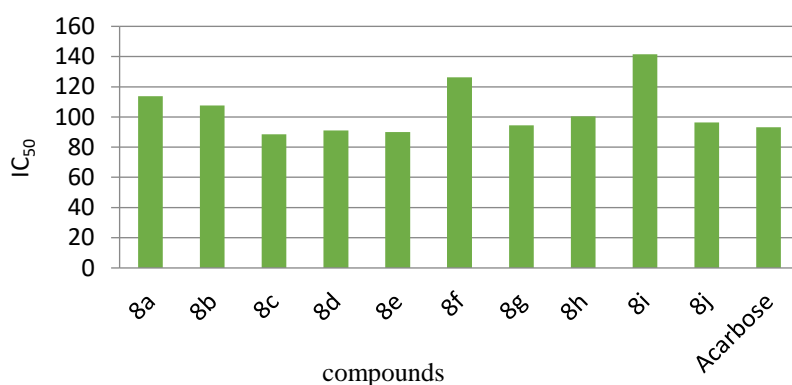


Figure 3. IC₅₀ values of compounds **8a-j**

3.3.7. Statistical Analysis of α -Glucosidase Inhibition Assay

The IC₅₀ values of compounds **8a-j** were measured in triplicate and statistically examined to assess their α -glucosidase inhibitory activity. To determine the overall significance of the differences between the compounds, a one-way ANOVA test was performed. For pairwise comparisons, Tukey's HSD post hoc test was then used. The ANOVA results confirmed that the compounds' inhibitory effects differed greatly, with a very significant variation among the investigated compounds ($F = 72557.92$, $p = 2.72 \times 10^{-47}$). Significant differences across several compound pairs were also found using Tukey's multiple comparison test, suggesting that some derivatives had significantly stronger or lower α -glucosidase inhibition than others. These variations are depicted in the box plot representation of IC₅₀ values (Figure 4), where compounds **8c**, **8e**, and **8d** exhibit the lowest IC₅₀ values and, consequently, the maximum inhibitory activity. Compound **8i**, on the other hand, showed the highest IC₅₀ value, suggesting a lower inhibition. The promise of these compounds as α -glucosidase inhibitors is further supported by the fact that the reference drug Acarbose showed inhibition comparable to several produced derivatives. These results emphasize that substituent alterations have a considerable impact on inhibitory potency and highlight the structure-activity correlations (SAR) among the produced compounds.

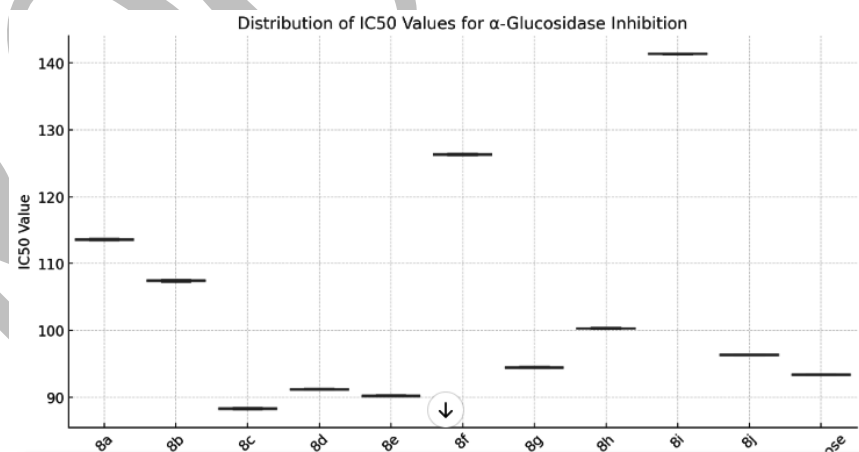


Figure 4. Box plot of IC₅₀ values for α -glucosidase inhibition

4. Conclusion

A novel and eco-friendly method has been developed for the synthesis of a series of new α -aminophosphonates (**8a-j**). This innovative approach uses nano-ZnO as an effective, reusable catalyst, minimizing waste and environmental impact. The solvent-free synthesis process, enhanced by microwave irradiation, achieves high yields through the K-F reaction mechanism. This strategy aligns with green chemistry principles by reducing the use of organic solvents and promoting efficient catalyst utilization. Molecular docking and ADMET simulations identified compounds with excellent drug-like properties, ensuring potential efficacy and safety. The synthesized compounds exhibited effective inhibition of the α -amylase enzyme, with compounds **8g**, **8i**, **8e**, and **8j** displaying greater potency than the reference drug. Future directions involve conducting in vivo studies to validate the in vitro findings, investigating the detailed mechanisms underlying α -amylase and α -glucosidase inhibition, and structurally modifying the compounds to enhance efficacy while minimizing potential side effects. The most promising candidates will be advanced toward clinical evaluation. Additionally, the potential of this green synthesis approach will be explored for the development of other pharmacologically important compounds. The environmentally friendly synthesis of compounds **8a-j**, supported by both computational and experimental validation, represents a significant advancement in the field of drug discovery. These compounds hold promise as next-generation anti-diabetic agents, offering potential advantages in terms of efficacy, safety, and environmental sustainability.

Acknowledgements

Authors acknowledge Dr. C. Naga Raju, Department of Chemistry, S. V. University, Tirupati for his constant support to complete this work.

Supporting Information

Supporting information accompanies this paper on <http://www.acgpubs.org/journal/organic-communications>

ORCID

A.Hanumantha Rao: [0000-0001-5371-5825](https://orcid.org/0000-0001-5371-5825)
Chennamsetty Subramanyam: [0000-0002-0422-6096](https://orcid.org/0000-0002-0422-6096)
K. Venkata Ramana: [0000-0002-4515-0796](https://orcid.org/0000-0002-4515-0796)
C Gladis Raja Malar: [0000-0001-8608-9023](https://orcid.org/0000-0001-8608-9023)
G.R. Satyanarayana: [0000-0002-6984-0003](https://orcid.org/0000-0002-6984-0003)
V. Madhava Rao: [0000-0002-0031-5200](https://orcid.org/0000-0002-0031-5200)

References

- [1] Krentz, A. J.; Bailey, C. Oral antidiabetic agents: current role in type 2 diabetes mellitus. *Drugs* **2005**, *65* (3), 385-411.
- [2] Chiasson, J.L. Acarbose for the prevention of diabetes, hypertension, and cardiovascular disease in subjects with impaired glucose tolerance: the study to prevent non- insulin-dependent diabetes mellitus (STOP-NIDDM) Trial. *Endocrin. Pract.* **2006**, *1*, 25-30.
- [3] Chen, X.; Zheng, Y.; Shen, Y. Voglibose (Basen, AO-128), One of the most important α -glucosidase inhibitors. *Curr. Med. Chem.* **2006**, *13*, 109-116.
- [4] Vora, J.; Patel, S.; Sinha, S. Advances in molecular docking as a tool for drug discovery and development. *Front. Pharmacol.* **2019**, *10*, 127.
- [5] Bagi, P.; Herbay, R.; Varga, B.; Fersch, D.; Fogassy, E.; Keglevich, G. The preparation and application of optically active organophosphorus compounds. *Phosphorus Sulfur Silicon Relat. Elem.* **2019**, *194*, 591-594.

- [6] Basha, S.T.; Sudhamani, H.; Rasheed, S.; Venkateswarlu, N.; Vijaya, T., Raju, C.N. Microwave-assisted neat synthesis of α -aminophosphonate/phosphinate derivatives of 2-(2-aminophenyl) benzothiazole as potent antimicrobial and antioxidant agents. *Phosphorus, Sulfur Silicon Relat. Elem.* **2016**, *191*, 1339-1343.
- [7] Shameem, M.A., Orthaber, A. Organophosphorus compounds in organic electronics. *Chem.Eur. J.* **2016**, *22*, 10718-10735.
- [8] Jean-Luc, M. Phosphinate chemistry in the 21st century: A viable alternative to the use of phosphorus trichloride in organophosphorus synthesis. *Acc. Chem. Res.* **2014**, *47*, 77-87.
- [9] Orsini, F.; Sello, G.; Sisti, M. Aminophosphonic acids and derivatives. Synthesis and biological applications. *Curr. Med. Chem.* **2010**, *17* (3), 264-289.
- [10] Dhawan, B.; Redmore, D. Optically active 1-aminoalkylphosphonic acids. *Phosphorus Sulfur Silicon Relat. Elem.* **1987**, *32*, 119-144.
- [11] Mucha, A.; Kafarski, P.; Berlicki, L. Remarkable potential of the α -aminophosphonate/phosphinate structural motif in medicinal chemistry. *J. Med. Chem.* **2011**, *54* (17), 5955-5980.
- [12] Mucha, A.; Kafarski, P.; Berlicki, L. Remarkable potential of the α -aminophosphonate/phosphinate structural motif in medicinal chemistry. *J. Med. Chem.* **2011**, *54*, 5955-5980.
- [13] Naydenova, E.D.; Todorov, P.T.; Troev, K.D. Recent synthesis of aminophosphonic acids as potential biological importance. *Amino Acids* **2010**, *38*, 23-30.
- [14] Bhattacharya, A.K.; Raut, D.S.; Rana, K.C.; Polanki, I.K.; Khan, M.S.; Iram, S.E. Diversity-oriented synthesis of α -aminophosphonates: a new class of potential anticancer agents. *J. Med. Chem.* **2013**, *66*, 146-152.
- [15] Huang, X. C.; Wang, M.; Pan, Y. M.; Yao, G. Y.; Wang, H. S.; Tian, X. Y.; Qin, J. K.; Zhang, Y. Synthesis and antitumor activities of novel thiourea α -aminophosphonates from dehydroabietic acid. *Euro. J. Med. Chem.* **2013**, *69*, 508-520.
- [16] Kafarski, P.; Lejczak, B. Aminophosphonic acids of potential medical importance. *Curr. Med. Chem. Anticancer Agent.* **2001**, *1*, 301-312.
- [17] Damiche, R.; Chafaa, S. Synthesis of new bioactive aminophosphonates and study of their antioxidant, anti-inflammatory and antibacterial activities as well the assessment of their toxicological activity. *J. Mol. Struct.* **2017**, *1130*, 1009-1017.
- [18] Sujatha, B.; Mohan, S.; Subramanyam, Ch.; Prasada Rao, K. Microwave-assisted synthesis and anti-inflammatory activity evaluation of some novel α -aminophosphonates. *Phosphorus, Sulfur Silicon Relat. Elem.* **2017**, *192* (3), 267-270.
- [19] Kuemin, M.; Donk, W.A. Structure-activity relationships of the phosphonate antibiotic dehydrophos. *Chem. Commun.* **2010**, *46*, 7694-7696.
- [20] Subramanyam, Ch.; Thaslim Basha, Sk.; Madhava, G.; Nayab Rasool, Sk.; Adam, Sk.; Durga Srinivasa Murthy S.; Naga Raju, C. Synthesis, spectral characterization and bioactivity evaluation of novel α -aminophosphonates. *Phosphorus, Sulfur Silicon Relat. Elem.* **2017**, *192* (3), 267-270.
- [21] Sarapuk, J.; Bonarska, D.; Kleszczyńska, H. Biological activity of binary mixtures of 2,4-D with some aminophosphonates. *J. Appl. Biomed.* **2003**, *1* (3), 169-173.
- [22] Yang, S.; Gao, X.W.; Diao, C.L.; Song, B.; Jing, L.H.; Xu, G.G.; et al., Synthesis and antifungal activity of novel chiral α -aminophosphonates containing fluorine moiety. *Chin. J. Chem.* **2006**, *24*, 1581-1588.
- [23] Herczegh, P.; Buxton, T.B.; McPherson, J.C.; Kova'cs-Kulyassa, A.; Brewer, P.D.; Sztaricskai, F.; Stroebel, G.G.; Plowman, K.M.; Farcasiu, D.; Hartmann, J.F. Osteo adsorptive bisphosphonate derivatives of fluoroquinolone antibacterials. *J. Med. Chem.* **2002**, *45* (11), 2338-2341.
- [24] Berlicki L., Kafarski P. Computer-Aided Analysis and Design of Phosphonic and Phosphinic Enzyme Inhibitors as Potential Drugs and Agrochemicals. *Curr. Org. Chem.* **2005**, *9*, 1829-1850.
- [25] Maheshwara Reddy, N.; Poojith, N.; Mohan, G.; Mohan Reddy, Y.; Saritha, V. K.; Visweswara Rao, P. Vijaya Kumar Reddy, A.; Swetha, V.; Grigory, V. Z.; Satheesh Krishna, B.; Suresh Reddy, C. Green Synthesis, Antioxidant, and Plant Growth Regulatory Activities of Novel α -Furfuryl-2-alkylaminophosphonates. *ACS Omega*, **2021**, *6* (4), 2934-2948.
- [26] Mohan, G.; Santhisudha, S.; Madhu Kumar Reddy, K.; Vasudeva Reddy, N.; Vijaya, T.; Suresh Reddy, C. Phosphosulfonic acid-catalyzed green synthesis and bioassay of α -aryl- α' -1,3,4-thiadiazolyl aminophosphonates. *Heteroat. Chem.* **2016**, 1-10.

Synthesis of α -aminophosphonates

- [27] Miller, D.J.; Hammond, S.M.; Anderluzzi, D.; Bugg, T.D.H. Aminoalkylphosphinate inhibitors of D-Ala-D-Ala adding enzyme. *J. Chem. Soc. Perkin Trans.* **1998**, *1*, 131-142.
- [28] Kuznetsov, Y.I.; Kazanskaya, G.Y.; Tsurulnikova, N.V. Aminophosphonate corrosion inhibitors for steel. *Prot. Met.* **2003**, *39*, 120-123.
- [29] Xie, D.; Zhang, A.; Liu, D.; Wan, J.; Zeng, S.; Hu, D. Synthesis and antiviral activity of novel α -aminophosphonates containing 6-fluorobenzothiazole moiety. *Phosphorus, Sulfur Silicon Relat. Elem.* **2017**, *192*, 1061-1067.
- [30] Subramanyam, Ch.; Kiran Kumar, K.; Venkata Ramana, K.; Gladis Raja Malar, C.; Mohan, S.; Mohan, S.; Nagalakshmi, V. Ultrasound mediated nano ZnO catalyzed synthesis of new α -aminophosphonates as potential anti-diabetic agents; an *in silico* ADMET, molecular docking study, α -amylase and α -glucosidase inhibitory activity, *Synth. Commun.* **2023**, *53* (23), 2041-2060.
- [31] Madhu Kumar Reddy, K.; Peddanna, K.; Varalakshmi, M.; Bakthavatchala Reddy, N.; Sravya, G.; Grigory, V. Z.; Suresh Reddy, C. Ceric ammonium nitrate (CAN) catalyzed synthesis and α -glucosidase activity of some novel tetrahydropyridine phosphonate derivatives. *Phosphorus, Sulfur Silicon Relat. Elem.* **2019**, *194*, 812-819.
- [32] Murali, S.; Venkataramaiah, C.; Saichaitanya, N.; Mohan, G.; Yasmin, S.H.; Rajendra, W.; Cirandur, S.R. Green synthesis, molecular docking, anti-oxidant and anti-inflammatory activities of α -aminophosphonates. *Med. Chem. Res.* **2019**, *28*, 1740-1754.
- [33] Sreelakshmi, P.; Nadiveedhi, M.R.; Santhisudha, S.; Mohan, G.; Saichaitanya, N.; Sadik, M.; Peddanna, K.; Cirandur, S.R. Nano Sb₂O₃ catalyzed green synthesis, cytotoxic activity, and molecular docking study of novel α -aminophosphonates. *Med. Chem. Res.* **2019**, *28*, 528-544.
- [34] Mohan, G.; Kumar, S.; Sudileti, M.; Sridevi, C.; Venkatesu, P.; Reddy, C.S. Excellency of pyrimidinyl moieties containing α -aminophosphonates over benzthiazolyl moieties for thermal and structural stability of stem bromelain, *Int. J. Biol. Macromol.* **2020**, *165* (B), 2010-2021.
- [35] Reddy, K.M.K.; Santhisudha, S.; Mohan, G.; Peddanna, K.; Rao, C.A.; Reddy, C.S. Nano Gd₂O₃ catalyzed synthesis and anti-oxidant activity of new α -aminophosphonates. *Phosphorus, Sulfur Silicon Relat. Elem.* **2016**, *191*, 933-938.
- [36] Ordonez, M.; Cabrera, H. R.; Cativiela, C. An overview of stereoselective synthesis of α -aminophosphonic acids and derivatives. *Tetrahedron* **2009**, *65*, 17-49.
- [37] Crooks, R.M.; Zhao, M.; Sun, L.; Chechik, V.; Yeung, L.K. Dendrimer-encapsulated metal nanoparticles: synthesis, characterization, and applications to catalysis, *Acc. Chem. Res.* **2001**, *34* (3), 181-190.
- [38] Bubun, B. Recent developments on nano-ZnO catalyzed synthesis of bioactive heterocycles. *J. Nanostructure Chem.* **2017**, *7*, 389-413.
- [39] Redjemia, R.; Berredjem, M.; Bahadi, R. Green and Cost-Effective Synthesis of Sulfamidophosphonates Using ZnO Nanoparticles as catalyst. *Eng. Proc.* **2023**, *37* (1), 98(1-6) .
- [40] Gourav, K.; Vijesh, T.; Parveen, K.; Meena, N. Zinc oxide nanoparticles as efficient heterogeneous catalyst for synthesis of bio-active heterocyclic compounds. *Chemistry Select* **2023**, *8*(41), e202303181, 1-37.
- [41] Safaei-Ghomi, J.; Ali Ghasemzadeh, Md. Zinc oxide nanoparticle promoted highly efficient one pot three-component synthesis of 2,3-disubstituted benzofurans. *Arab. J. Chem.* **2017**, *10* (2), S1774-S1780.
- [42] Harshita, S.; Rekha S. ZnO Nanoparticles as an efficient, heterogeneous, reusable, and ecofriendly catalyst for four-component one-pot green synthesis of pyranopyrazole derivatives in water. *Sci. World J.* **2013**, *2013*(1), 1-8.
- [43] Satish Kumar, N.; Sameer Reddy, M.; Vema Reddy, B.; Saratchandra Babu, M.; Raju Chowhan, L. Chandrasekhara Rao, L. Zinc oxide nanoparticles as efficient catalyst for the synthesis of novel di-spiroindolizidine bisoxindoles in aqueous medium. *Environ. Chem. Lett.* **2019**, *17*, 455-464.
- [44] Redjemia, R.; Berredjem, M.; Bahadi, R. Green and cost-effective synthesis of sulfamidophosphonates using ZnO nanoparticles as Catalyst. *Eng. Proc.* **2023**, *37*(1), 98.
- [45] Elham, E. Green synthesis of α -aminophosphonates using ZnO nanoparticles as an efficient catalyst. *Z. Naturforsch. B.* **2018**, *73* (3-4), 179-184.

- [46] Thaslim Basha, SK.; Rasheed, S.; Chandra Sekhar, K.; Naga Raju, C.; Subhan Ali Md.; Appa Rao Ch. Ultrasonicated, nano-ZnO catalyzed green synthesis of α -hydroxyphosphonates and their antioxidant activity, *Phosphorus Sulfur Silicon Relat. Elem.* **2014**, 189 (10), 1546-1556.
- [47] Subramanyam, CH.; Kiran Kumar, K.; Venkata Ramana, K.; Gladis Raja Malar, C.; Mohan, S.; Nagalakshmi, V. Ultrasound mediated nano-ZnO catalyzed synthesis of new α -aminophosphonates as potential anti-diabetic agents; An *in silico* ADMET, molecular docking study, α -amylase and α -glucosidase inhibitory activity. *Synth. Commun.* **2023**, 53 (23), 2041-2060.
- [48] Mohan, G.; Santhisudha, S.; Madhu Kumar Reddy, K.; Vasudeva Reddy, N.; Vijaya, T.; Suresh Reddy, C. Phosphosulfonic acid-catalyzed green synthesis and bioassay of α -aryl- α' -1,3,4-thiadiazolyl aminophosphonates. *Heteroat. Chem.* **2016**, 27, 1-10.
- [49] De la Hoz, A.; Draz Ortiz, A.; Moreno, A. Microwaves in organic synthesis. Thermal and non-thermal microwave effects. *Chem. Soc. Rev.* **2005**, 34, 164-178.
- [50] Vorathavorn, V. I.; Sykes, J. E.; Feldman, D. G.; Vet, J. Cryptococcosis as an emerging systemic mycosis in dogs. *J. Vet. Emerg. Crit. Care.* **2013**, 23, 489-497.
- [51] Shiro, T.; Fukaya, T.; Tobe, M. The chemistry and biological activity of heterocycle-fused quinolinone derivatives: a review. *Eur. J. Med. Chem.* **2015**, 97, 397-408.
- [52] Altaff, SK. Md.; Raja Rajeswari, T.; Subramanyam, Ch. Synthesis, α -amylase inhibitory activity evaluation and *in silico* molecular docking study of some new phosphoramidates containing heterocyclic ring. *Phosphorus, Sulfur Silicon Relat. Elem.* **2021**, 196 (4), 389-397.
- [53] Pavan Phani Kumar, M.; Anuradha, V.; Subramanyam, Ch.; Hari Babu, V. *In silico* molecular docking study, synthesis and α -amylase inhibitory activity evaluation of phosphorylated derivatives of purine. *Phosphorus, Sulfur Silicon Relat. Elem.* **2021**, 196 (11), 1010-1017.
- [54] Hanumantha Rao, A.; Madhava Rao, V.; Subramanyam, Ch.; Priyadarshini, P.; Someswara Rao, S.; Visweswara Rao, P. An *in silico* ADMET, molecular docking study and microwave-assisted synthesis of new phosphorylated derivatives of thiazolidinedione as potential anti-diabetic agents. *Synth. Comm.* **2022**, 52 (2), 300-315.
- [55] Sujatha, B.; Subramanyam, Ch.; Venkataramaiah, Ch.; Rajendra W.; Prasada rao, K. Synthesis and anti-diabetic activity evaluation of phosphonates containing thiazolidinedione moiety. *Phosphorus, Sulfur Silicon Relat. Elem.* **2020**, 195 (7), 586-591.
- [56] Bozdag-Dünder, O.; Verspohl, E.J.; Daş-Evcimen, N.; Kaup, R.M.; Bauer, K.; Sarikaya, M.; Evranos, B.; Ertan, R. Synthesis and biological activity of some new flavonyl-2,4-thiazolidinediones. *Bioorg. Med. Chem.* **2008**, 16 (14), 6747-6751.
- [57] Mori, M.; Takagi, M.; Noritake, C.; Kagabu, S. 2,4-Dioxo-1,3-thiazolidine derivatives as a lead for new fungicides. *J. Pestic. Sci.* **2008**, 33, 357-363.
- [58] Ceriello, A. Thiazolidinediones as anti-inflammatory and anti-atherogenic agents. *Diabetes Metab. Res. Rev.* **2008**, 24 (1), 14-26.
- [59] Eun, J.S.; Kim, K.S.; Kim, H.N.; Park, S.A.; Ma, T.Z.; Lee, K.A. et al. Synthesis of psoralen derivatives and their blocking effect of hKv1.5 channel. *Arch. Pharm. Res.* **2007**, 30 (2), 155-160.
- [60] Sahu, S.K.; Banerjee, M.; Mishra, S.K.; Mohanta, R.K.; Panda, P.K.; Misro, P.K. Synthesis, partition coefficients and antibacterial activity of 3'-phenyl (substituted)-6' aryl-2' (1H)-cis-3',3'-a-dihydrospiro [3-H-indole-3,5'-pyrazolo (3',4'-d)-thiazolo-2-(1H) ones]. *Acta Pol. Pharm.* **2007**, 64 (2), 121-126.
- [61] Angajala, G.; Subashini, R.; Sebastian, M. Review on Novel 2,4-Thiazolidinedione Derivatives as Potential Therapeutic Agents for Type II Diabetes. *Diabetes Mellitus and Human Health Care*, **2014**, 229-246.
- [62] Yoshioka, T.; Fujita, T.; Kanai, T.; Aizawa, Y.; Kurumada, T.; Hasegawa, K.; Horikoshi, H. Studies on hindered phenols and analogues. 1-Hypolipidemic and hypoglycemic agents with ability to inhibit lipid peroxidation. *J. Med. Chem.* **1989**, 32 (2), 421-428.
- [63] Altaff, SK. Md.; Raja Rajeswari, T.; Subramanyam, Ch. Synthesis, α -amylase inhibitory activity evaluation and *in silico* molecular docking study of some new phosphoramidates containing heterocyclic ring. *Phosphorus, Sulfur Silicon Relat. Elem.* **2021**, 196 (4), 389-397.

Synthesis of α -aminophosphonates

- [64] Pavan Phani Kumar, M.; Anuradha, V.; Subramanyam Ch.; Hari Babu, V. V. In silico molecular docking study, synthesis and α -amylase inhibitory activity evaluation of phosphorylated derivatives of purine. *Phosphorus, Sulfur Silicon Relat. Elem.* **2021**, *196* (11), 1010-1017
- [65] Sujatha, B.; Subramanyam, Ch.; Venkataramaiah, Ch.; Rajendra, W.; Prasada rao, K. Synthesis and anti-diabetic activity evaluation of phosphonates containing thiazolidinedione moiety. *Phosphorus, Sulfur Silicon Relat. Elem.* **2020**, *195* (7), 586-591.
- [66] Vijay, M.P.; Kalpana, N.T.; Neha, M. U.; Ramaa C. S. Synthesis, In-Vitro Evaluation and Molecular Docking Study of *N*-Substituted Thiazolidinediones as α -Glucosidase Inhibitors. *Chemistry Select.* **2022**, *7*, 1-11.
- [67] Ramandeep, K.; Rajnish, K.; Nilambra, D.; Ashok, K.; Ashok Kumar, Y.; Manoj, K. Synthesis and studies of thiazolidinedione-isatin hybrids as α -glucosidase inhibitors for management of diabetes. *Future Med. Chem.* **2021**, *13* (5), 1-5.
- [68] Wang, G.; Peng, Y.; Xie, Z.; Wang, J.; Chen, M. Synthesis, α -glucosidase inhibition and molecular docking studies of novel thiazolidine-2,4-dione or rhodanine derivatives. *Med. Chem. Comm.* **2017**, *8*, 1477-1484.
- [69] Hidalgo-Figueroa, S.; Ramirez-Espinosa, J.J.; Estrada-Soto, S.; Almanza-Pérez, J. C.; Román-Ramos, R.; Alarcón-Aguilar, F.J. *et al.* Discovery of thiazolidine-2,4-dione/biphenylcarbonitrile hybrid as dual PPAR α/γ modulator with antidiabetic effect: *in vitro*, *in silico* and *in vivo* approaches. *Chem. Biol. Drug Des.* **2013**, *81*, 474-483.
- [70] Kaur, J.; Singh, A.; Singh, G.; Verma, R.K.; Mall, R. Novel indolyl linked *para*-substituted benzyldiene-based phenyl containing thiazolidinediones and their analogs as α -glucosidase inhibitors: synthesis, *in vitro*, and molecular docking studies. *Med. Chem. Res.* **2018**, *27*, 903-914.
- [71] Senthil kumar, N.; Vijaya kumar, V.; Sarveswari, S.; Sarveshwari, G.A.; Gayathri, M. Synthesis of new thiazolidine-2,4-dione-azole derivatives and evaluation of their α -amylase and α -glucosidase inhibitory activity. *Iran. J. Sci. Technol. Trans. Sci.* **2019**, *43*, 735-745.
- [72] Ravikumar, D.; Mohan, S.; Subramanyam, Ch.; Prasada Rao, K. Solvent-Free Sonochemical Kabachnic-Fields Reaction To Synthesize Some New α -Aminophosphonates Catalyzed By Nano-BF₃ SiO₂. *Phosphorus, Sulfur Silicon Relat. Elem.* **2018**, *193* (6), 400-407.
- [73] Sujatha, B.; Mohan, S.; Subramanyam, Ch.; Prasada Rao, K. Microwave-assisted synthesis and anti-inflammatory activity evaluation of some novel α -aminophosphonates. *Phosphorus, Sulfur Silicon Relat. Elem.* **2017**, *192* (3), 267-270.
- [74] Subramanyam, Ch.; Taslim bhasha, SK.; Madhava, G.; Adam, SK.; Srinivasa Murthy, S. D.; Naga Raju, C. Synthesis, spectral characterization and bioactivity evaluation of novel α -aminophosphonates. *Phosphorus, Sulfur Silicon Relat. Elem.* **2017**, *192* (3), 267-270. DOI:
- [75] Haji basha, M.; Subramanyam, Ch.; Prasada rao, K. Ultrasound-promoted solvent-free synthesis of some new α -aminophosphonates as potential antioxidants. *Main group met. Chem.* **2020**, *43*, 147-153.
- [76] Prashantha Kumar, B.R.; Soni, M.; Kumar, S.S.; Singh, K.; Patil, M.; Baig, R.B.N.; Laxmi, A. Synthesis, glucose uptake activity and structure-activity relationships of some novel glitazones incorporated with glycine, aromatic and alicyclic amine moieties via two carbon acyl linker. *Eur. J. Med. Chem.* **2011**, *46*, 835-844.
- [77] Young, M. H.; Yun Jung, P.; Jin-Ah, K.; Daeui, P.; Ji Young, P.; Hye Jin, L. *et al.* Design and synthesis of 5-(substituted benzyldiene)thiazolidine-2,4-dione derivatives as novel tyrosinase inhibitors. *Eur. J. Med. Chem.* **2012**, *49*, 245-252;
- [78] Moghaddam, F. M.; Saeidian, H.; Mirjafary, Z.; Sadeghi, A. Rapid and efficient one-pot synthesis of 1,4-dihydropyridine and polyhydroquinoline derivatives through the Hantzsch four component condensation by zinc oxide. *J. Iran. Chem. Soc.* **2009**, *6*, 317-324.
- [79] Shantikumar, N.; Abhilash, S.; Divya Rani, V. V.; Deepthy, M.; Seema, N.; Manzoor, K.; Satish, R. Role of size scale of ZnO nanoparticles and microparticles on toxicity toward bacteria and osteoblast cancer cells. *J. Mater. Sci.: Mater. Med.* **2009**, *20*, S235-241
- [80] Madhu Kumar Reddy, K.; Mohan, G.; Bakthavatchala Reddy, N.; Sravya, G.; Peddanna, K.; Grigory, V. Z.; Sridevi, C.; Suresh Reddy, C. Synthesis, antioxidant activity, and α -glucosidase enzyme inhibition of α -aminophosphonate derivatives bearing piperazine-1,2,3-triazole moiety. *J. Heterocycl. Chem.* **2021**, *58*, 172-181.

- [81] Priyadarsini, P.; Madhava Rao, V.; Hanumatha Rao A.; Subramanyam Ch.; Ranganayakulu Y. A simple, efficient synthesis and molecular docking studies of 2-styrylchromones. *Org. Commun.* **2021**, *14* (2), 121-132.
- [82] Haji Basha, M.; Subramanyam, Ch.; Gladis Raja Malar, C.; Someswara Rao, S.; Prasada Rao, K. Nano TiO₂.SiO₂ catalyzed, microwave assisted synthesis of new α -aminophosphonates as potential anti-diabetic agents: In silico ADMET and molecular docking study. *Org. Commun.* **2022**, *15* (2), 167-183.
- [83] Terry, R. S.; James, R. K.; Stephen, R.J.; Xue-Qing C.; Arthur, D.; Yi, Li. *In Silico* ADME/Tox: Why Models Fail. *J. Comput. Aid. Mol. Des.* **2003**, *17* (2-4), 83-92.
- [84] Tingjun, H.; Junmei W.; Wei, Z.; Xiaojie X. ADME Evaluation in Drug Discovery. 6. Can Oral Bioavailability in Humans Be Effectively Predicted by Simple Molecular Property-Based Rules? *J. Chem. Inf. Model.* **2007**, *47* (2), 460-463.
- [85] Trudy, R.; David, L. Physiologically Based Pharmacokinetic Modeling 1: Predicting the Tissue Distribution of Moderate-to-Strong Bases. *J. Pharm. Sci.* **2005**, *94* (6), 1259-1276.
- [86] Daina, A.; Zoete, V. A boiled-egg to predict gastrointestinal absorption and brain penetration of small molecules. *Chem. Med. Chem.* **2016**, *11*, 1117-1121.
- [87] Montanari, F.; Ecker, G. F. Prediction of drug-ABC-transporter interaction-recent advances and future challenges. *Adv. Drug Deliv. Rev.* **2015**, *86*, 17-26.
- [88] Hollenberg, P. F. Characteristics and common properties of inhibitors, inducers, and activators of CYP enzymes. *Drug Metab. Rev.* **2002**, *34*, 17-35.
- [89] Shiew-Mei, H.; John, M. S.; Lei, Z.; Kellie, S. R.; Srikanth, N.; Robert, T. *et al.* New era in drug interaction evaluation: US food and drug administration update on CYP enzymes, transporters, and the guidance process. *J. Clin. Pharmacol.* **2008**, *48*, 662-670.
- [90] Potts, R. O.; Guy, R. H. Predicting Skin Permeability. *Pharm. Res.* **1992**, *9*, 663-669.
- [91] Lipinski, C.A.; Lombardo, F.; Dominy, B.W.; Feeney, P.J. Experimental and computational approaches to estimate solubility and permeability in drug discovery and development settings. *Adv. Drug Del. Rev.* **2001**, *46*, 3-26.
- [92] Ghose, A.K.; Viswanadhan, V.N.; Wendoloski, J.J. Prediction of hydrophobic (lipophilic) properties of small organic molecules using fragmental methods: An analysis of ALOGP and CLOGP methods. *J. Phys. Chem. A.* **1998**, *102*, 3762-3772.
- [93] Veber, D.F.; Johnson, S.R.; Cheng, H.Y.; Smith, B.R.; Ward, K.W.; Kopple, K.D. Molecular properties that influence the oral bioavailability of drug candidates. *J. Med. Chem.* **2002**, *45*, 2615-2623.
- [94] Egan, W.J.; Lauri, G. Prediction of intestinal permeability. *Adv. Drug Del. Rev.* **2002**, *54*, 273-289.
- [95] Muegge, I.; Heald, S.L.; Brittelli, D. Simple selection criteria for drug-like chemical matter. *J. Med. Chem.* **2001**, *44*, 1841-1846.
- [96] Trott, O.; Olson, A.J. Auto Dock Vina: improving the speed and accuracy of docking with a new scoring function, efficient optimization and multithreading. *J. Comput. Chem.* **2010**, *31*, 455-461.
- [97] Nickavar, B.; Amin, G. Enzyme assay guided isolation of an alpha-amylase inhibitor flavonoid from vaccinium arctostaphylos leaves. *Iran J. Pharm. Res.* **2011**, *10*, 849-853.
- [98] Patil, V. S.; Nandre, K. P.; Ghosh, S.; Rao, V. J.; Chopade, B. A.; Sridhar, B.; Bhosale, S. V.; Bhosale, S. V. Synthesis, crystal structure and anti-diabetic activity of substituted (E)-3-(benzo[d]thiazol-2-ylamino)phenylprop-2-en-1-one. *Eur. J. Med. Chem.* **2013**, *59*, 304-309.
- [99] Kim, J.S.; Hyun, T.K.; Kim, M.J. The inhibitory effects of ethanol extracts from sorghum, foxtail millet and proso millet on α -glucosidase and α -amylase activities. *Food Chem.* **2011**, *124*, 1647-1651.